European Journal of Radiology 112 (2019) 169–179

Contents lists available at ScienceDirect

European Journal of Radiology

journal homepage: www.elsevier.com/locate/ejrad

Research article

MRI texture analysis based on 3D tumor measurement reflects the IDH1 mutations in gliomas – A preliminary study

Liang Han[a], Siyu Wang[b], Yanwei Miao[a,*], Huicong Shen[c,**], Yan Guo[d], Lizhi Xie[e], Yuqing Shang[f], Junyi Dong[a], Xiaoxin Li[a], Weiwei Wang[a], Qingwei Song[a]

[a] Department of Radiology, The First Affiliated Hospital of Dalian Medical University, Dalian 116000, China
[b] College of medical imaging, Dalian Medical University, Dalian, 116044, China
[c] Department of Radiology, Beijing Tian Tan Hospital, Capital Medical University, Beijing, 100050, China
[d] Life science, GE Healthcare, Shenyang, 110000, China
[e] GE Healthcare, MR Research China, Beijing, China
[f] Department of Chronic Disease Epidemiology, Yale School of Public Health, Yale University, New Haven, Connecticut, USA

ARTICLE INFO

Keywords:
Magnetic resonance imaging
Isocitrate dehydrogenase 1
Gliomas

ABSTRACT

Objective: To evaluate the differentiation efficiency of texture analysis of T1WI, T2WI and contrasted-enhanced T1WI MRI sequences in gliomas with and without IDH1 mutation based on entire tumor region.

Materials and methods: A total of 42 patients with histopathologically confirmed gliomas, including 21 patients carrying IDH1 mutation ($IDH1^{mutation}$ group) and 21 with wild-type IDH1 ($IDH1^{wt}$ group) were included in this study. The preoperative MRI and clinical data were collected. The regions of interest (ROIs) covering the entire tumor and edema were manually delineated on axial slices using O.K. (Omni Kinetics, GE Healthcare, China) software; and the histogram and GLCM features based on T1WI, T2WI and contrasted-enhanced T1WI sequences were automatically generated.

Results: Based on contrasted-enhanced T1WI features, the inertia resulted as the best feature for diagnosis, with the AUC of 0.844. Furthermore, the AUC for gliomas prediction with $IDH1^{mutation}$ was 0.800 for cluster prominence. IDH1-mutation was differentiated on T2WI with the highest AUC of 0.848, which corresponded to GLCM Entropy. After modeling, the accuracy of the contrasted-enhanced T1WI, T1WI, and T2WI features model was 0.952, 0.857, and 0.738, respectively. The AUC of Joint $Variable_{T1WI+C}$ for predicting $IDH1^{mutation}$ was 0.984, while the AUC of Joint $Variable_{T1WI}$ for predicting the same mutation was 0.927. The diagnostic efficiency of Joint $Variable_{T2WI}$ was also desirable.

Conclusion: MRI texture analysis could be used as a new noninvasive method for identification of gliomas with IDH1 mutation. The present results show that the Joint Variable derived from conventional MR imaging histogram and GLCM features is suitable for precise detection of IDH1-mutated gliomas.

1. Introduction

Previous studies have shown that patients with IDH1-mutated gliomas have improved prognosis compared to those with wild-type IDH1 gliomas [1,2]. At present, the IDH gene can only be detected following surgery or biopsy. Recent studies have shown that IDH1 mutation may serve as a predictive biomarker that can be used to guide aggressive surgical resection without enhancing tumor margins [3]. In addition, the mutation status of the IDH1 gene has a very important clinical significance for the selection of individual therapy for patients with glioma. Bujko et al. [4] have found that the drug sensitivity to temozolomide in patients with gliomas is associated with the presence of the mutation in the IDH1. Accordingly, it is necessary to predict the mutation of IDH1.

Abbreviations: MRI, magnetic resonance imaging; IDH1, isocitrate dehydrogenase 1; ROIs, regions of interest; GLCM, gray-level co-occurrence matrix; RMS, root mean square; AUC, area under the curve; SD, standard deviation; ADC, apparent diffusion coefficient; FSE, fast spin echo; Gd DTPA, gadolinium-DTPA; DICOM, digital imaging and communications in medicine; ICC, intra-class correlation coefficients; PHD, prolyl hydroxylase; 2-HG, 2-hydroxyglutaric acid; HIF-1a, hypoxia-inducible factor 1-alpha

* Corresponding author at: Department of Radiology, The First Affiliated Hospital, Dalian Medical University, Liaoning, 116011, China.
** Corresponding author at :Department of Radiology, Beijing Tian Tan Hospital, Capital Medical University, Beijing, 100050, China.
E-mail addresses: hl0912postgraduate@163.com (L. Han), 1051845992@qq.com (S. Wang), ywmiao716@163.com (Y. Miao), shenhuicong@126.com (H. Shen).

https://doi.org/10.1016/j.ejrad.2019.01.025
Received 9 September 2018; Received in revised form 10 January 2019; Accepted 22 January 2019

So far, conventional magnetic resonance imaging (MRI) has been used as an indispensable method for noninvasive diagnosis and prognosis evaluation of glioma. Genomic changes in glioma are related to some of the imaging features of MRI [5]. Xiong et al. [6] have found that the ADC value is different for oligodendrocytoma carrying IDH1 mutation compared to those with wild-type IDH1 using diffusion tensor imaging. Furthermore, Yamashita et al. [7] have suggested that TBF calculated from ASL and tumor necrosis area, derived from conventional MR imaging, are useful for predicting the IDH1 mutation status. However, the exact prediction of the IDH1 mutation through observation of the conventional MRI images with naked eye is very limiting.

Texture analysis is an image post-processing technology that uses mathematical methods to analyze the distribution and arrangement of all the pixels in the medical images and has a series of quantitative features. MRI texture analysis is based on the comprehensive analysis of signal intensity of each imaging sequence. Multi-features can comprehensively reflect the intrinsic microscopic pathological characteristics of tumors, which then can be used to diagnose or evaluate the prognosis. So far, there are only few studies on the conventional magnetic resonance texture analysis of IDH mutation status in glioma. Bisdas et al. [8] have used texture analysis and support vector machine based on diffusional kurtosis imaging to predict glioma grade and IDH mutation. Furthermore, Jakola et al. [9] have used Haralick texture parameters based on preoperative clinical FLAIR sequence to predict the IDH status in low-grade gliomas. In this study, we used texture analysis of T1WI, T2WI and contrast enhanced T1WI sequences to predict the IDH1 mutation in low grade and high-grade gliomas based on 3D tumor measurements.

2. Materials and methods

2.1. Patients

The local institutional review board approved this retrospective study. We reviewed glioma cases who underwent surgical reaction at the Neurosurgical Center between January 2016 and September 2017. A total of 42 cases, including 21 IDH1 mutants ($IDH1^{mutation}$; 11 males, 10 females, mean age ± standard deviation (SD) = 43.81 ± 10.79 years) and 21 IDH1 wild-types ($IDH1^{wt}$; 10 males, 11 females, mean age ± SD = 56.95 ± 10.94 years) with complete IDH1 genetic information and MR data were included in the study. All cases were divided into two groups according to the eventual presence of IDH1 mutation. The clinical data and tumor characteristics between the two groups are summarized in Table 1.

2.2. MRI protocol

MRI was performed using 3.0 T MR scanner (Signa HDxt, General Electric Co., Milwaukee, WI, USA) with a standard head coil. The following MR sequence was applied: sagittal and axial fast spin echo (FSE) T1WI, axial fast spin echo (FSE) T2WI. After injection of Gadolinium (Gd DTPA: 0.1 mmol/kg of body weight, rate of 3.0 ml/s), contrasted T1-weighted images were acquired, which included three-dimensional structure imaging (3D Brain Volume) and axial FSE T1WI. MRI protocol is shown in Table 2.

2.3. Image post-processing

The Digital Imaging and Communications in Medicine (DICOM) format data of T1WI, T2WI and contrast enhanced T1WI sequences were transferred to the personal computer, and image post-processing based on the corresponding signal intensity map was carried out using O.K. (Omni Kinetics, GE Healthcare, China) software. Two radiologists, who were blind to the grouping, manually analyzed the regions of interest (ROIs) on all axial slices of the T1WI, T2WI and contrasted enhanced T1WI maps, respectively. ROIs covered all the tumor parenchyma and the edema regions, which were suspected of the presence of cystic lesion, necrosis or bleeding (Fig. 1).

For tumors with clear boundaries, ROI was easy to determine, and there were gliomas with blurred boundaries and large edema areas. T2WI has great advantages for determining ROI range of edema, and contrasted enhanced T1WI is very important in determining ROI range of tumor parenchyma. Therefore, in the process of delineating ROI, radiologists refer to the enhanced images of T2WI and contrasted enhanced T1WI to determine the delineation of edema and tumor parenchyma, so as to ensure the ROI consistency of the three sequences. The ROIs at all levels of T1WI sequence were accumulated to 3D ROI. Similarly, the 3D ROI of T2WI sequence and contrasted enhanced T1WI sequence were obtained by the same method. The features of three sequences of 3D ROI were automatically extracted using the software.

Twenty-nine features were generated automatically, including first-order histogram features (minIntensity, maxIntensity, meanvalue, standard deviation, variance, volume count, root mean square (RMS), range, mean deviation, relative deviation, skewness, kurtosis, uniformity, energy, entropy, quantile5, quantile10, quantile25, quantile50, quantile75, quantile90, quantile95) and second-order Gray-Level Co-occurrence Matrix (GLCM) features (GLCM energy, GLCM entropy, inertia, correlation, inverse difference moment, cluster shade, cluster prominence). The features are shown in Fig. 2.

2.4. Data analysis

All the statistical analyses were performed in language R (RStudio Version 1.0.143–© 2009–2016 RStudio, Inc.). $P < 0.05$ was considered statistically significant. Intra-class correlation coefficients (ICC) were used for the consistency assessment between radiologists.

2.4.1. Statistical comparison between IDH1-mutated and IDH1-WT group

For the data that conformed to normal distribution, student *t*-test was used; otherwise, the-rank-sum test was performed. Receiver operating characteristic (ROC) curve was plotted to assess the differential diagnostic efficiency of the significant features.

Table 1
Baseline characteristics between the two groups.

Parameters \ group	Total	IDH1-mutation	IDH1-WT	*P*
Sex (males/females, No.)	42	11/10	10/11	0.758
Age (Mean ± SD years)	-	43.81 ± 10.79	56.95 ± 10.94	0
Grade WHO IV glioblastoma No. (%)	14(33%)	0	14(33%)	0
Grade WHO III oligodendroid astrocytoma	4(10%)	4(10%)	0	0.035
Grade WHO III oligodendrocytoma	6(14%)	3(7%)	3(7%)	1.000
Grade WHO III anaplastic astrocytoma	6(14%)	5(12%)	1(2%)	0.078
Grade WHO III ganglioglioma	1(2%)	0	1(2%)	0.311
Grade WHO II oligodendroid astrocytoma	2(5%)	2(5%)	0	0.147
Grade WHO II oligodendrocytoma	3(7%)	3(7%)	0	0.072
Grade WHO II astrocytoma	6(14%)	4(10%)	2(5%)	0.378

Table 2
MRI protocol.

Sequences	TR (ms)	TE (ms)	Section thickness (mm)	Intersection gap (mm)	FOV (cm × cm)	Matrix
T1WI	300-400	9	6.0	1.0	22.0 × 22.0	288 × 192
T2WI	3000-4000	110	6.0	1.0	22.0 × 22.0	320 × 256
3D BRAVO	8.3	3.1	1.2	0	25.6 × 20.5	320 × 256

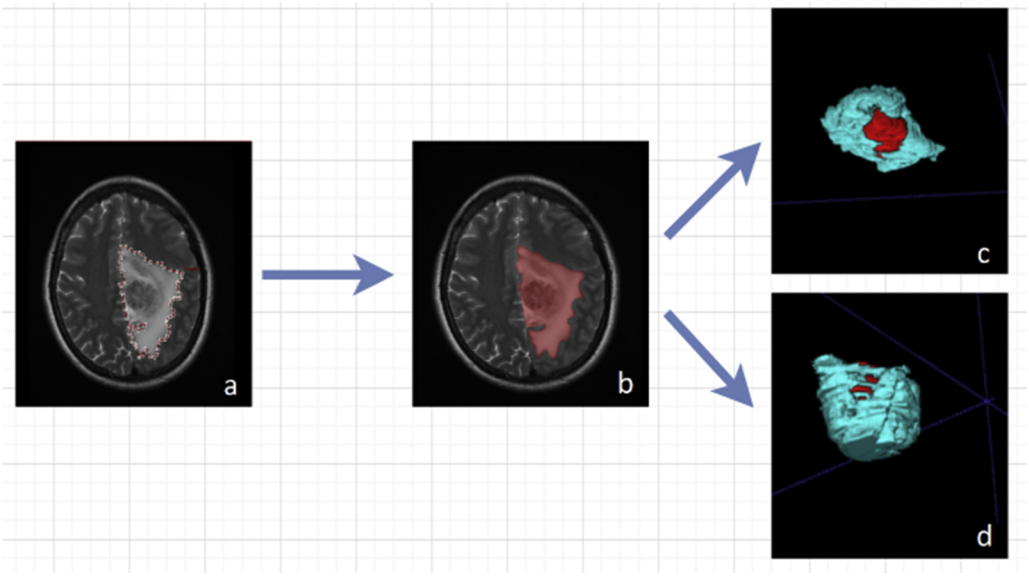

Fig. 1. (a) A T2WI image generated by Omni-Kinetics software to depict ROI of the tumor. (b) 3D ROI image of tumor (red area) that is calculated to superimpose at all levels in the T2WI map. (c-d) A three-dimensional image of the tumor. The red represents the substantial part of the tumor, and the blue indicates the edema around the tumor.

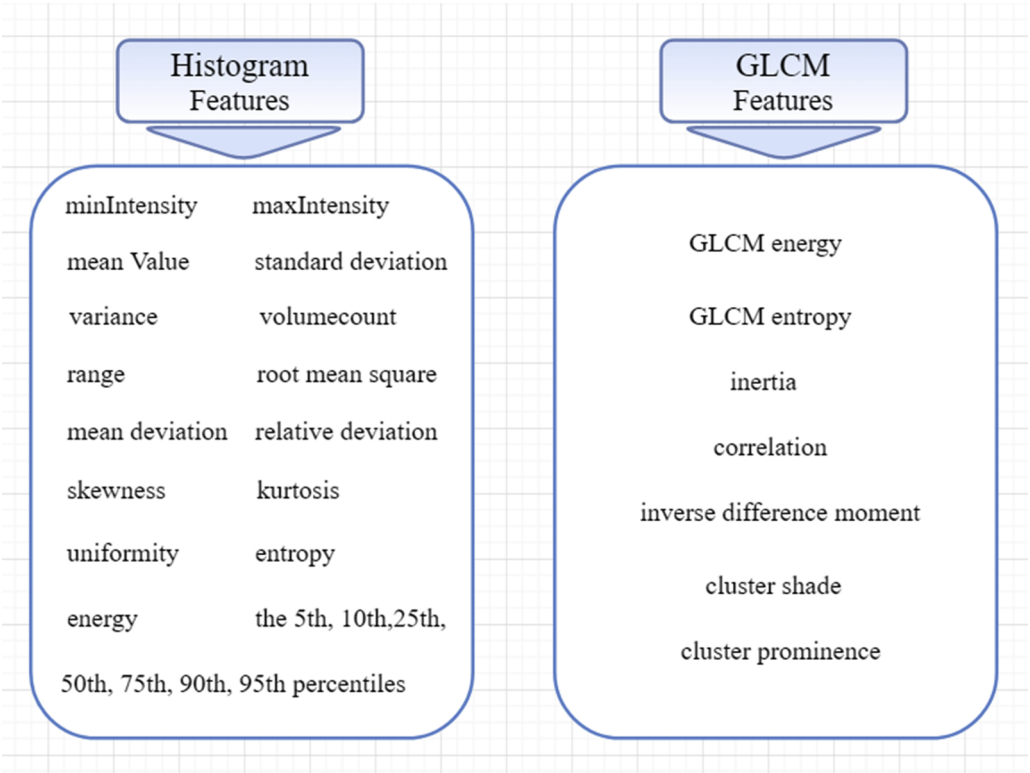

Fig. 2. A total of 29 Histogram and GLCM features.

2.4.2. Logistic regression model

After dimension reduction, features with statistical significance were selected ($P < 0.05$). The correlation coefficient was set to 0.9. Spearman analysis was used to eliminate the features with the correlation coefficients higher than 0.9. Logistic regression analysis was used to establish the model with meaningful features. Confusion matrix was used to analyze the accuracy of the model. ROC curve was plotted to assess the differential diagnostic efficiency of the features after

Table 3
Histogram and GLCM features extracted from contrast enhanced T1WI.

Features(T1WI + C)	IDH1-mutation(n = 21)	IDH1-WT(n = 21)	*P* value
MinIntensity	(0.16 ± 0.11)×10^3	(0.27 ± 0.16)×10^3	0.023 #
*stdDeviation	(0.16 ± 0.15)×10^3	(0.26 ± 0.16)×10^3	0.005 #
*Variance	(0.25 ± 0.49)×10^5	(0.69 ± 0.86)×10^5	0.005 #
skewness	0.50 ± 0.70	1.31 ± 0.82	0.001 #
*uniformity	0.84 ± 0.14	0.70 ± 0.09	0.000 #
GLCM Entropy	4.37 ± 0.80	4.88 ± 0.59	0.033 #
Inertia	2.32 ± 1.80	4.41 ± 2.01	0.000 #
Correlation	0.31 ± 0.19	0.14 ± 0.07	0.000 #
InverseDifferenceMoment	0.66 ± 0.07	0.61 ± 0.07	0.048 #
*ClusterShade	4.62 ± 27.90	61.28 ± 73.06	0.003 #
*ClusterProminence	(0.17 ± 0.32) ×10^3	(0.87 ± 0.88) ×10^3	0.000 #

Note: The previous standard * indicates the abnormal distribution, express with (median ± interquartile range), and others are normal distribution, express with (mean value ± standard deviation), the right side is marked # indicates P < 0.05, with statistically significant differences.

Table 4
Histogram and GLCM features extracted from T1WI.

Features(T1WI)	IDH1-mutation(n = 21)	IDH1-WT(n = 21)	*P* value
MinIntensity	(0.18 ± 0.11)×10^3	(0.30 ± 0.15)×10^3	0.011 #
* GLCM Energy	0.05 ± 0.03	0.03 ± 0.02	0.004 #
* GLCM Entropy	4.91 ± 0.79	5.79 ± 0.87	0.001 #
* Inertia	2.65 ± 1.13	5.88 ± 4.71	0.004 #
* Correlation	0.18 ± 0.11	0.08 ± 0.09	0.008 #
InverseDifferenceMoment	0.59 ± 0.06	0.53 ± 0.09	0.005 #
*ClusterProminence	(0.314 ± 0.312)×10^3	(1.09 ± 2.07)×10^3	0.000 #

Note: The previous standard * indicates the abnormal distribution, express with (median ± interquartile range), and others are normal distribution, express with (mean value ± standard deviation), the right side is marked # indicates P < 0.05, with statistically significant differences.

Table 5
Histogram and GLCM features extracted from T2WI.

Features(T2WI)	IDH1-mutation(n = 21)	IDH1-WT(n = 21)	*P* value
*stdDeviation	(0.33 ± 0.23) ×10^3	(0.60 ± 0.34) ×10^3	0.005 #
*Variance	(1.12 ± 1.73) ×10^5	(3.63 ± 3.60) ×10^5	0.005 #
*kurtosis	3.16 ± 1.52	2.32 ± 1.10	0.001 #
*uniformity	0.77 ± 0.07	0.71 ± 0.12	0.006 #
* Quantile75	(1.52 ± 1.16) ×10^3	(2.20 ± 1.42) ×10^3	0.015 #
Quantile90	(1.99 ± 0.73) ×10^3	(2.68 ± 1.01) ×10^3	0.021 #
Quantile95	(2.17 ± 0.78) ×10^3	(2.84 ± 1.09) ×10^3	0.034 #
*GLCM Energy	0.05 ± 0.02	0.03 ± 0.01	0.000 #
*GLCM Entropy	5.13 ± 0.44	5.87 ± 0.55	0.000 #
* Inertia	3.40 ± 1.95	6.34 ± 4.02	0.000 #
* Correlation	0.14 ± 0.10	0.07 ± 0.05	0.000 #
InverseDifferenceMoment	0.58 ± 0.04	0.53 ± 0.06	0.000 #
* ClusterProminence	(0.52 ± 0.62)×10^3	(1.50 ± 3.29)×10^3	0.005 #

Note: The previous standard * indicates the abnormal distribution, express with (median ± interquartile range), and others are normal distribution, express with (mean value ± standard deviation), the right side is marked # indicates P < 0.05, with statistically significant differences.

modeling (Joint Variable).

3. Results

3.1. Difference of histogram and GLCM features between two groups (independent variable)

The ICC values of all patients with gliomas were > 0.8. In texture analysis of contrasted-enhanced T1WI features, minIntensity, standard deviation, variance, skewness, GLCM entropy, inertia, cluster shade and cluster prominence were significantly increased; while uniformity, correlation and inverse difference moment were significantly decreased in $IDH1^{wt}$ group compared to $IDH1^{mutation}$ group (all P < 0.05). According to ROC analysis, the inertia (area under the curve (AUC) = 0.844) was considered the best parameter for the diagnosis of $IDH1^{wt}$ and $IDH1^{mutation}$ gliomas, with the sensitivity of 85.7% and specificity of 81%, respectively. In addition, the $IDH1^{wt}$ gliomas revealed higher values for minIntensity, GLCM entropy, inertia, cluster prominence; and lower values of GLCM energy, correlation, inverse difference moment compared to $IDH1^{mutation}$ gliomas (all P < 0.05). The AUC of T1WI features for predicting IDH1 mutation was 0.800 for cluster prominence (specificity of 81% and sensitivity of 76.2%). In the T2WI features, standard deviation, variance, quantile75, quantile90, quantile95, GLCM entropy, Inertia and cluster prominence were all increased, while kurtosis, uniformity, GLCM energy, correlation, inverse difference moments were decreased in $IDH1^{wt}$ compared to $IDH1^{mutation}$ (all *P* < 0.05). IDH1-mutation was differentiated on T2WI with highest AUC = 0.848, sensitivity = 90.5%, specificity = 81% corresponding to GLCM Entropy (Tables 3–5; Figs. 5–7). The cases and histograms of $IDH1^{mutation}$ and $IDH1^{wt}$ are shown in Figs. 3 and 4.

3.2. Results of logistic regression model (Joint Variable)

We first selected the statistically significant features (P < 0.05) and

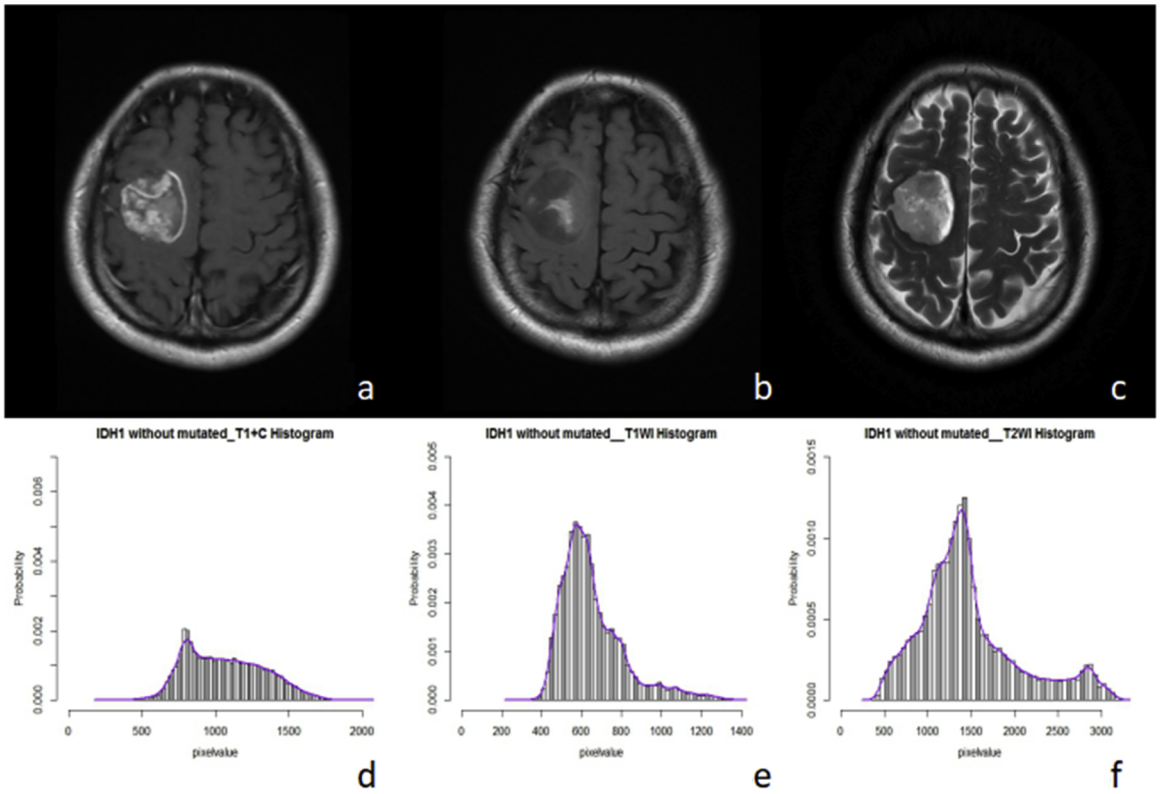

Fig. 3. A single case - a male patient, 60 years old, diagnosed with WHO III anaplastic astrocytoma carrying IDH1^{wt}. (a–c) Contrasted-enhanced T1WI, T1WI, T2WI signal images. The signal was slightly higher on T2WI and was low on T1WI. The signal was nonuniform, significantly enhanced and strengthening uniformity. (d–f) Contrasted-enhanced T1WI, T1WI, T2WI signal histograms. Centered on the spike, the voxel distribution on the right side of the peak is larger than that on the left side. It shows that all three histogram sequences of IDH1^{wt} group were rightward and the voxel value distribution in the high value area. In contrasted-enhanced T1WI, the curve of IDH1^{wt} was obviously flat compared to IDH1^{mutation}. In T1WI, the curve peak of IDH1^{wt} was lower compared to IDH1^{mutation}. In T2WI, the general trend of the curve was slightly slow.

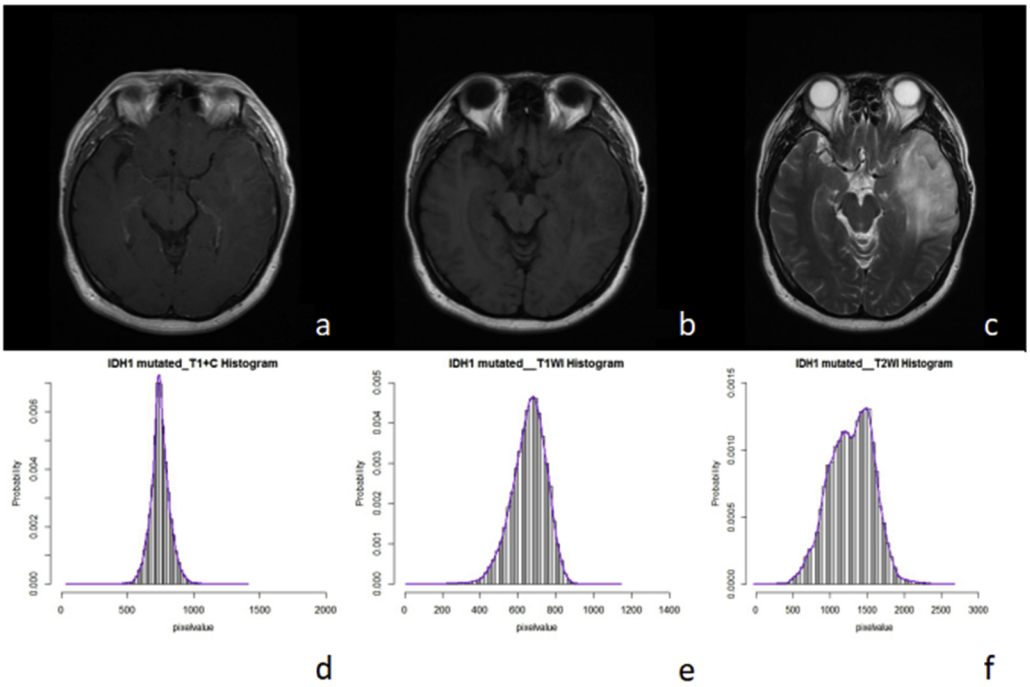

Fig. 4. A single case - a male patient, 31 years old, with WHO II Oligodendrocytes carrying IDH1^{mutation}. (a–c) Contrasted T1WI, T1WI, T2WI signal images. The signal was high on T2WI and was low on T1WI. The signal was homogeneous, slightly enhanced. (d–f) Contrasted T1WI, T1WI, T2WI signal histograms. Centered on the spike, the voxel distribution on the left side of the peak is larger than that on the right side. It shows that All three histogram sequences of IDH1^{mutation} group histogram were leftward, the voxel value distribution in the low value area. In contrasted-enhanced T1WI, the curve of IDH1^{wt} had an obviously high tip compared to IDH1^{mutation}. In T1WI, the curve peak of IDH1-mutated was higher compared to IDH1^{wt}. In T2WI, the general trend of the curve was relative centralization.

analyzed the redundant data. Then, we deleted the features with correlation coefficient > 0.9. In contrasted-enhanced T1WI sequences, the modeling features included the MinIntensity, Variance, Skewness, Correlation, Inverse Difference Moment, Cluster Shade, Cluster Prominence; in T1WI sequences, the features included the MinIntensity, Entropy, Inverse Difference Moment, Cluster Prominence; and in T2WI sequences, the modeling features included the Kurtosis, Uniformity, Quantile95, Correlation, Inverse Difference Moment and Cluster

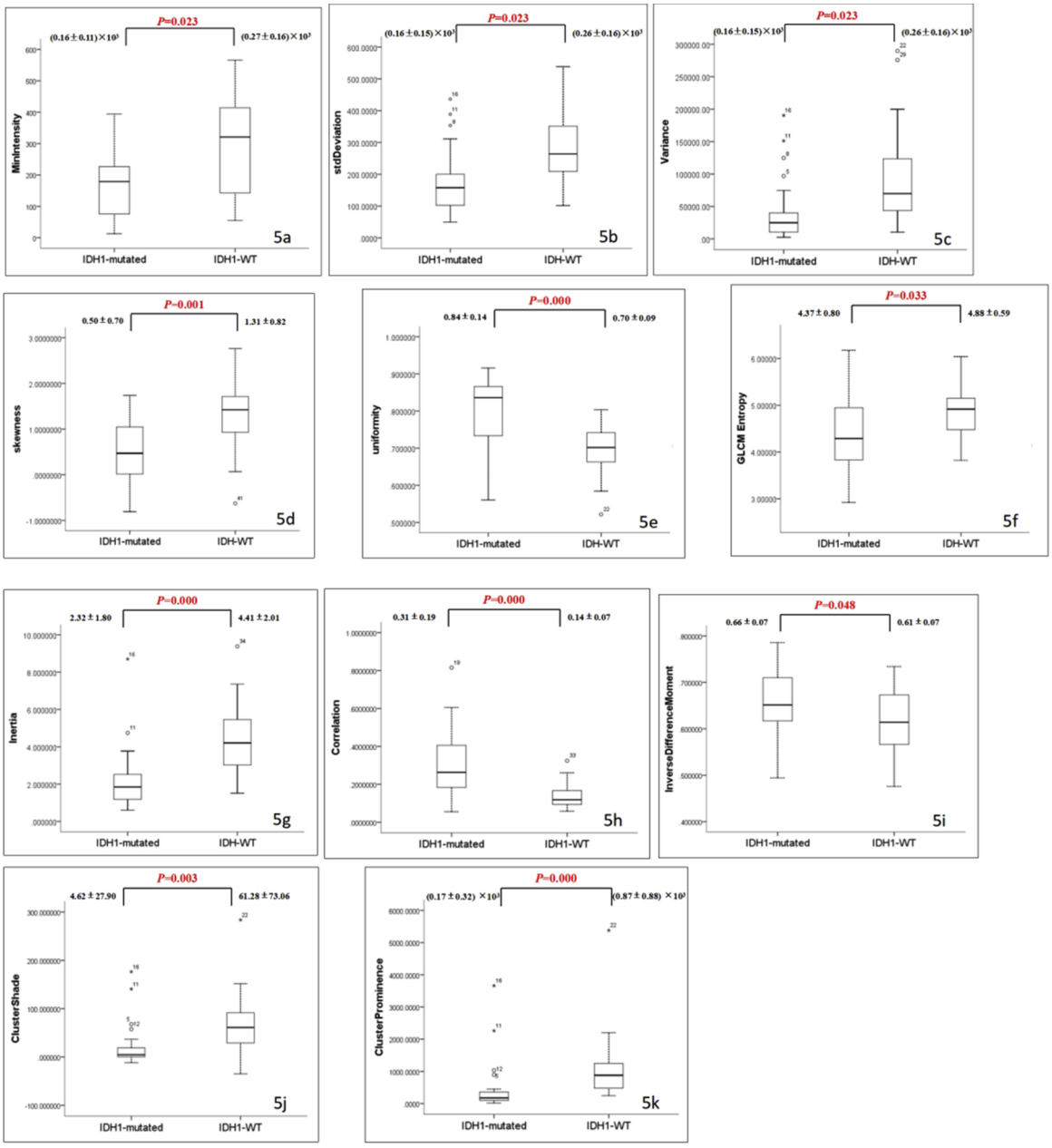

Fig. 5. Box diagrams of histogram and GLCM features extracted from contrast enhanced statistically significant T1WI ($p < 0.05$(Red font)).

Prominence.

The formulas for modeling contrasted-enhanced T1WI, T1WI, and T2WI are as follows:

$f_{T1WI} = 22.89 + 9.74e\text{-}3 \times \text{MinIntensity} - 2.97 \times \text{Entropy} - 22.08 \times \text{Inverse Difference Moment} + 3.4e\text{-}3 \times \text{Cluster Prominence}$

$f_{T1WI+C} = -46.4 + 1.97e\text{-}2 \times \text{MinIntensity} - 8.50e\text{-}7 \times \text{Variance} + 11.1 \times \text{skewness} - 1.75e+2 \times \text{Correlation} + 1.09e+02 \times \text{Inverse Difference Moment} - 41.9 \times \text{Cluster Shade} + 5.56e\text{-}4 \times \text{Cluster Prominence}$

$f_{T2WI} = 32.6 - 0.96 \times \text{kurtosis} - 11.2 \times \text{uniformity} + 6.22e\text{-}4 \times \text{Quantile95} + 41.3 \times \text{Correlation} - 51.3 \times \text{Inverse Difference Moment} + 5.56e\text{-}4 \times \text{Cluster Prominence}$

Coefficient of features of the contrasted-enhanced T1WI, T1WI and T2WI are shown in Table 6. The accuracy of the contrasted T1WI features, T1WI and T2WI model was 0.952, 0.857 and 0.738, respectively (Fig. 9). The contrasted-enhanced T1WI features model had the best accuracy. According to ROC analysis, the AUC of Joint Variable_{T1WI+C} for predicting $IDH1^{mutation}$ gliomas was 0.984 (cutoff value = 0.409, specificity of 90.5% and sensitivity of 100%), while the AUC of Joint Variable_{T1WI} for predicting gliomas with same mutation was 0.927 (cutoff value = 0.459, specificity of 90.5% and sensitivity of 90.5%). The diagnosis efficiency of Joint Variable_{T2WI} was also desirable. The AUC of Joint Variable_{T2WI} was 0.887 with the highest specificity of 95.2% (cutoff value = 0.632), and the highest sensitivity of 90.5% (cutoff value = 0.300) (Fig. 8).

4. Discussion

IDH1 genotyping is an important factor for predicting survival and prognosis of patients with glioma. Previous studies [1,10,11] have shown that the mutation of IDH1 is positively correlated with glioma prognosis. The mechanism of IDH1 mutation is mainly regulated by the metabolite 2-hydroxyglutaric acid (2-HG). Accumulation of metabolite

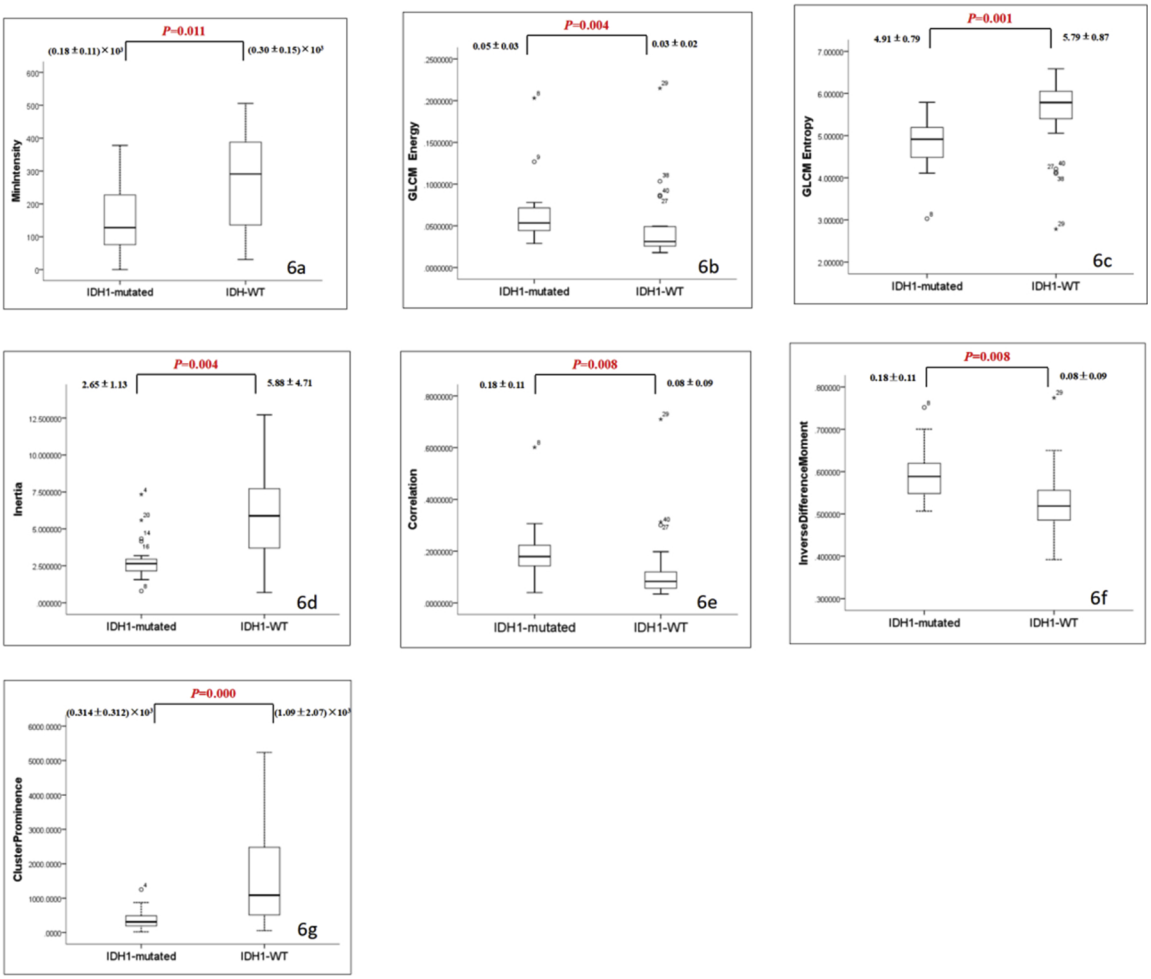

Fig. 6. Box diagrams of histogram and GLCM features extracted from statistically significant T1WI ($p < 0.05$ (Red font)).

2-HG produced by IDH1 mutation can cause abnormal histone and DNA methylation [12,13]. It can also lead to the increase of hypoxia-inducible factor 1-alpha (HIF-1a) and the activation of downstream genes [12] that has an important role in the pathophysiological process of glioma occurrence and development [14,15], such as tumor cell density, cell atypia, neovascularization and so on. In this study, texture analysis was used based on 3D tumor measurement. The measurement area included the whole tumor area, including the necrotic cystic area, hemorrhagic foci, the structure and edema area of tumor, thus providing more information about the tumor tissue. We have extracted the multi-texture features of the whole tumor region to comprehensively reflect the intrinsic microscopic pathological characteristics of tumors, and to predict the mutation of IDH1.

According to research, contrasted-enhanced T1WI features indicated that minIntensity, standard deviation, variance, skewness, GLCM entropy, inertia, clustershade and cluster prominence were significantly higher in $IDH1^{wt}$ compared to $IDH1^{mutation}$ gliomas. MinIntensity is the smallest value of the voxels in the ROI. The smallest intensification value of $IDH1^{wt}$ was increased compared to $IDH1^{mutation}$, indicating that the intensification of $IDH1^{wt}$ gliomas was greater than the intensification of gliomas carrying IDH1 mutation. Skewness describes the curve distribution of the histogram; it represents the degree of asymmetric image histogram distribution, and it can reflect the heterogeneity of the tumor [16–18]. If the skewness of the curve is deviated to the left side, this means that the distribution asymmetry tends to have a smaller value and that more voxels are concentrated in the low value area, while the deviation to the right indicates that the distribution asymmetry tends to have a larger value. In this study, we found a decreased skewness in $IDH1^{mutation}$ glioma compared to $IDH1^{wt}$ glioma. It is possible that the intensification of $IDH1^{mutation}$ glioma was lower, and so the voxel value of IDH1 mutation was distributed in the low value area. Moreover, Minintensity and skewness both indicated that the intensification of IDH1-mutated declined.

Wang et al. [19] have found that IDH1-mutated anaplastic gliomas are less likely to show contrast enhancement on MR images compared with tumors without IDH1 mutation. This is consistent with our study results. Nevertheless, some studies [14,20] have shown that the number of microvessels in IDH1-expressing tumor is significantly increased. 2-HG can inhibit the activity of PHD, stabilize the HIF-1a, increase the level of vascular endothelial growth factor, and further promote the proliferation of tumor vessels [1,21], which further suggest that the mutation of IDH1 is positively correlated with tumor angiogenesis. These data are contradictory to our results.

The enhancement of brain tumors depends on the extent of the destruction of blood supply and blood-brain barrier, and the conventional enhancement mainly reflects the destruction of blood-brain barrier [22]. The destruction of blood-brain barrier in glioma occurs due to the erosion of normal capillaries during the growth of tumors. IDH1 mutant glioma has a better prognosis. This suggests that glioma carrying an IDH1 mutation are less invasive than IDH1 wild-type gliomas and have a relatively lower degree of damage to blood-brain barrier. This pathological basis may explain our findings. Dynamic contrast-enhanced MR perfusion imaging can better reflect the perfusion of tumors and the proliferation of blood vessels, which is a new research direction.

Standard deviation and variance are used to evaluate the degree of

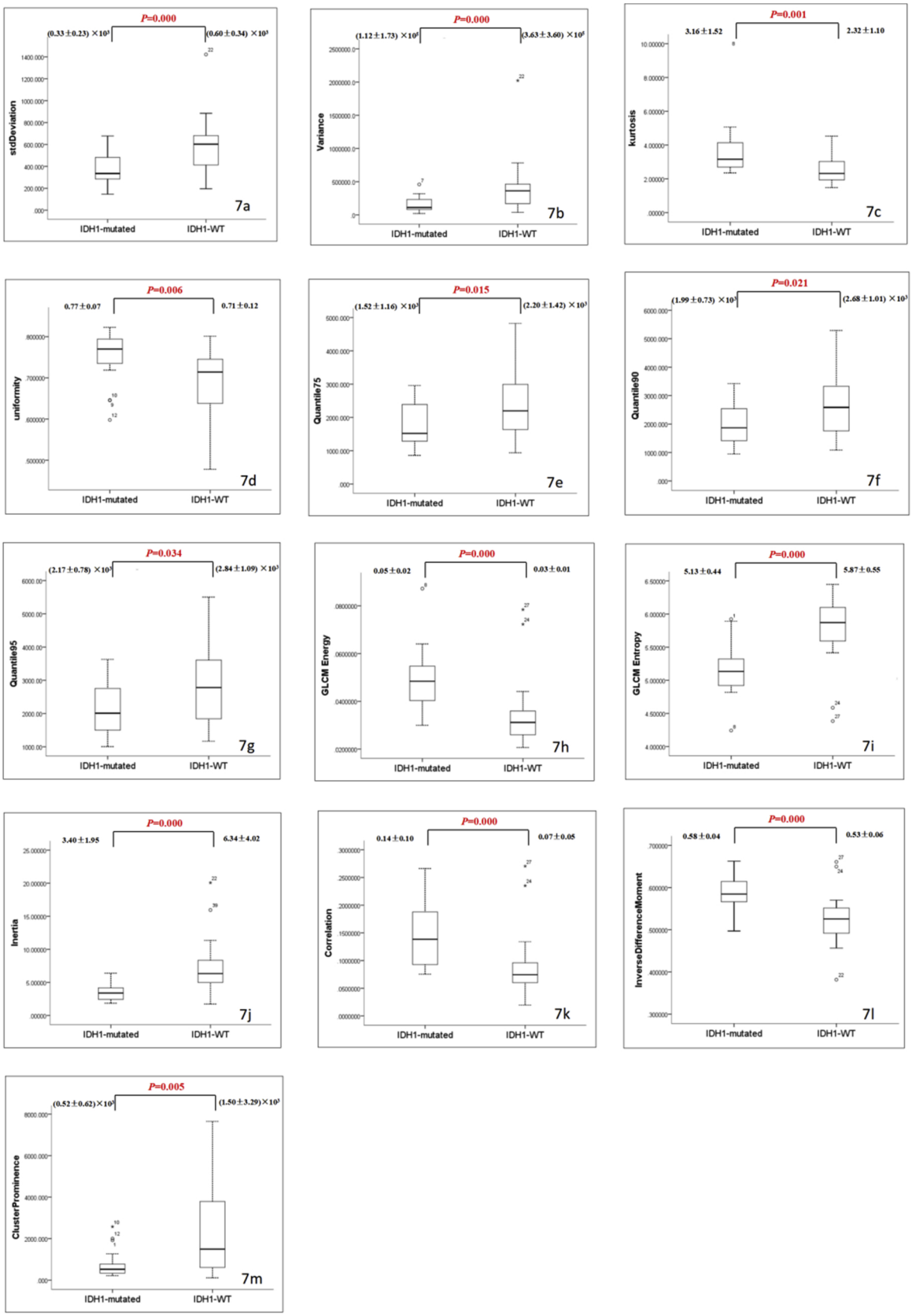

Fig. 7. Box diagrams of histogram and GLCM features extracted from statistically significant T2WI ($p < 0.05$(Red font)).

data dispersion. In contrasted-enhanced T1WI and T2WI features, the standard deviation and variance of IDH1^{wt} were higher compared to IDH1^{mutation}. With the increase of standard deviation, most of the data deviated from the mean value, indicating that the lesions were not uniform and enhancing the inhomogeneity. Previous studies [23] have shown that IDH1 mutation is closely related to the invasion of glioma.

Table 6
Results of logistic regression model.

	Features Coefficient	Estimate	Std. Error	z value	Pr(> |z|)
Contrast Enhanced T1WI	Intercept	−4.64e+01	3.78e+01	−1.23	0.219
	Min Intensity	1.97e-02	1.32e-02	1.50	0.134
	Variance	−8.50e-07	3.34e-05	−0.03	0.980
	skewness	1.11e+01	446.68e+00	1.66	0.097
	Correlation	−1.75e+02	1.19e+02	−1.47	0.142
	Inverse Difference Moment	1.09e+02	8.55e+01	1.27	0.203
	Cluster Shade	−4.19e-01	2.99e-01	−1.40	0.161
	Cluster Prominence	1.60e-02	1.34e-02	1.19	0.233
T1WI	Intercept	22.88894	15.20629	1.51	0.132
	Min Intensity	0.00974	0.00407	2.39	0.017 *
	Entropy	−2.97284	1.62173	−1.83	0.067
	Inverse Difference Moment	−22.08023	14.46589	−1.53	0.127
	Cluster Prominence	0.00340	0.00143	2.37	0.018 *
T2WI	Intercept	3.26e+01	1.84e+01	1.78	0.075
	kurtosis	−9.56e-01	5.90e-01	−1.62	0.105
	uniformity	−1.12e+01	1.14e+01	−0.98	0.326
	Quantile95	6.22e-04	4.99e-04	1.25	0.213
	Correlation	4.13e+01	2.71e+01	1.52	0.127
	Inverse Difference Moment	−5.13e+01	2.91e+01	−1.76	0.078
	Cluster Prominence	5.56e-04	7.11e-04	0.78	0.434

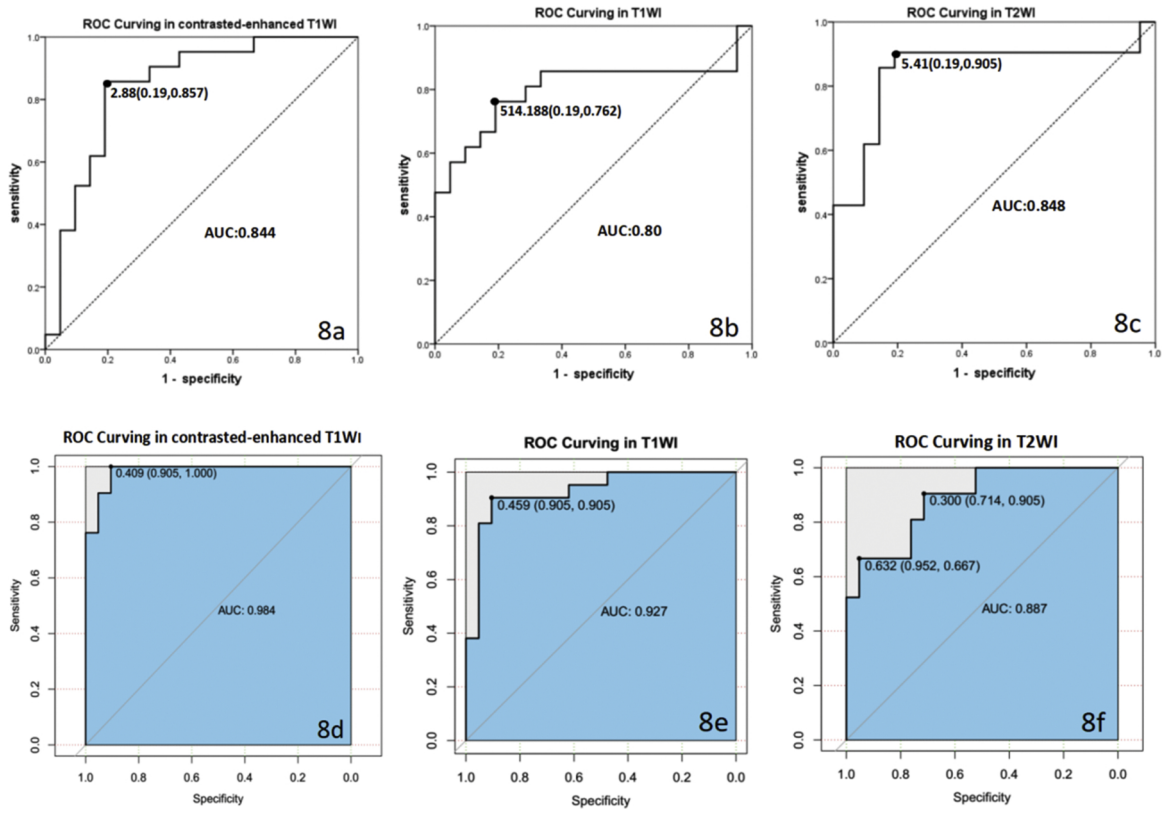

Fig. 8. (a–c) ROC curve (white background) of independent variable in contrasted T1WI, T1WI, T2WI. (d–f) ROC curve (blue background) of joint variables in contrasted T1WI, T1WI, T2WI. The sensitivity and specificity of joint variables were higher compared to independent variable.

IDH1 mutation can inhibit the HIF-1a pathway, reduce the adhesion spot, and then impair the migration and invasion ability of malignant cells. IDH1 wild-type glioma grows rapidly and is prone to hemorrhage, necrosis and cystic degeneration, which leads to nonuniform tumors. According to T1WI and T2WI features, GLCM energy of $IDH1^{mutation}$ gliomas is larger. The energy value reflects the uniformity of the gray distribution in the image and the roughness of the texture. The energy indicates that the texture is regular and stable. It also shows that the image signal of $IDH1^{mutation}$ is more homogeneous. According to T2WI features, quantile75, quantile90, quantile95 of $IDH1^{wt}$ were more meaningful for the diagnosis between the two types.

Significant difference of GLCM entropy, inertia, cluster prominence, correlation, and inverse difference moment were found between $IDH1^{mutation}$ and $IDH1^{wt}$ group. Increased GLCM entropy, inertia, and cluster prominence were observed in $IDH1^{wt}$ gliomas. The entropy shows the complexity of the image gray distribution. It also reflects the relationship between the clarity and the depth of the grooves. The texture of the groove gets deeper with the greater contrast, while the effect appears clear. The high value of cluster prominence shows that the gray value of the image is larger, and the difference of gray level

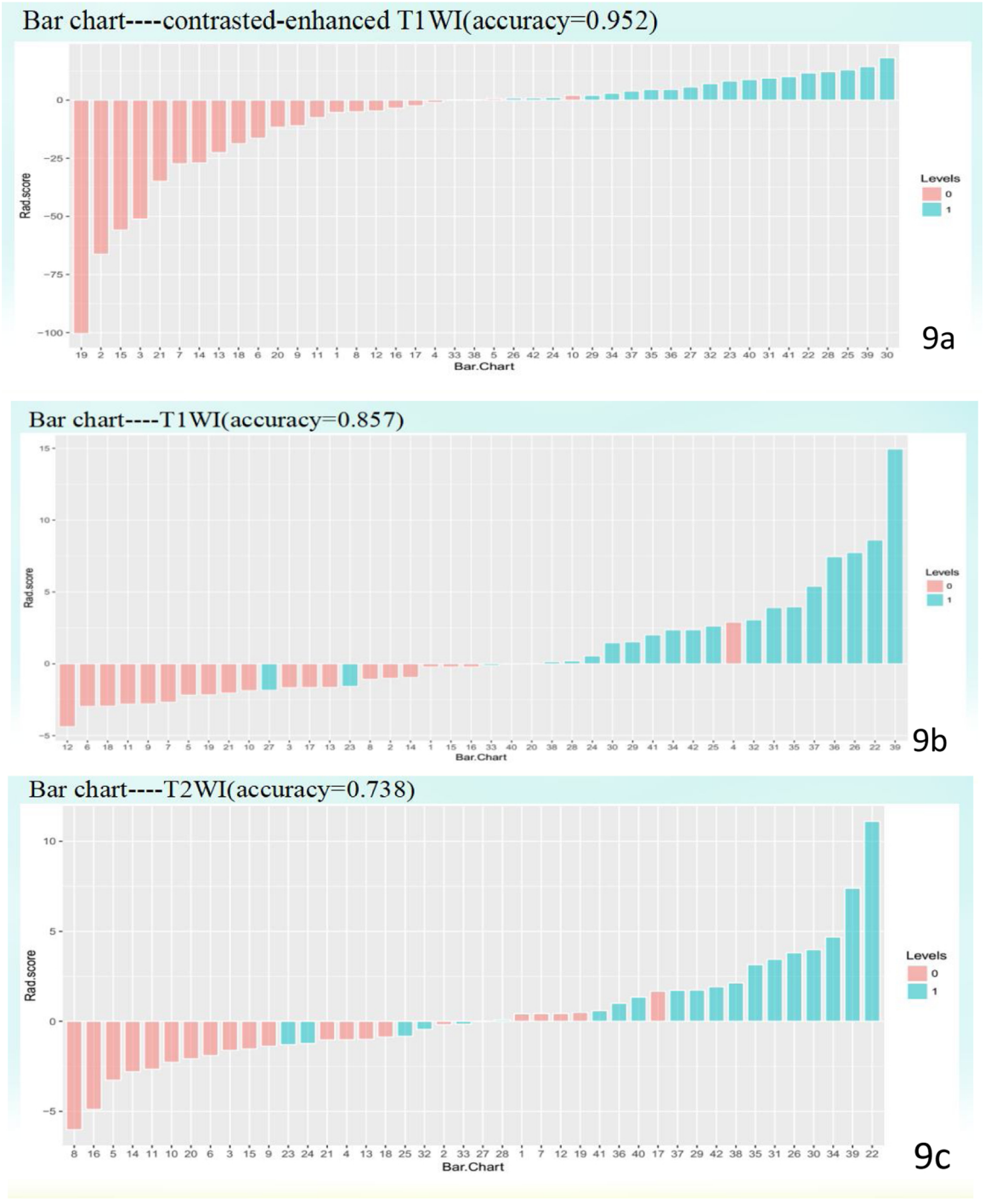

Fig. 9. The X-axis represents each patient, each bar represents one patient, the blue bar represents the IDH1 wild type, and the pink represents the IDH1 mutation type. 0 in ordinate was the threshold of model classification, that was the best diagnostic cut-off point. Bar charts of contrasted-enhanced T1WI, T1WI and T2WI. The accuracy of the contrasted T1WI, T1WI, T2WI features model was 0.952, 0.857, 0.738,respectively.

between different tissues is larger. In addition, the correlation and inverse difference of $IDH1^{wt}$ were lower compared to $IDH1^{mutation}$. The correlation reflects the correlation of local gray level, whereas the greater value stands for the greater correlation. The inverse difference moment reflects the homogeneity and the local change of the image texture. The large value indicates that there is no change between the different regions of the image texture, while the part is very homogeneous. Among them, GLCM entropy, and cluster prominence are equal to the heterogeneity of tumor. The heterogeneity of $IDH1^{wt}$ is higher, while the homogeneity is higher in $IDH1^{mutation}$, which is consistent with our results. In addition, we found that GLCM entropy and cluster prominence may all be related to the good prognosis of patients with $IDH1^{mutation}$. Regarding the T2WI features, the GLCM entropy had the highest diagnostic efficiency between the two groups, with the sensitivity of 90.5% and specificity of 81%, followed by inertia in the contrasted-enhanced T1WI with the sensitivity of 85.7% and specificity of 81%.

According to logistic regressions model, the contrasted-enhanced T1WI features model had the highest accuracy and the best diagnostic efficiency. The accuracy was up to 95.2%, and the sensitivity and

specificity were up to 100%, 95.2%, respectively. The accuracy (92.7%), sensitivity (90.5%) and specificity (90.5%) of the T1WI features model were next to the contrasted T1WI features model. This indicates that the logistic regressions models built with no more than seven features is not only interpretable but also discriminative. Furthermore, both contrast-enhanced T1WI and T1WI image sequences contribute comparatively to the differentiation of gliomas with and without IDH1 mutation and thereby, one imaging sequence can be curbed and the medical resource can be made the most use of. In addition, the number of patient cases is small due to high cost in the collection of genetic information and high-quality MR images. due to the limited sample size in current study, no validation methods were performed. Future studies should confirm the effectiveness of the model using forward-looking samples as independent validation groups.

5. Limitations

This study has some limitations. 1) More features were restricted due to the imbalance of the sample size and the number of features. 2) For the validation of logistic regression model, future studies should confirm the effectiveness of the model using forward-looking samples as independent validation groups. 3) Although the measurement area included the whole tumor area (necrotic cystic area, hemorrhagic foci, the structure and edema area of tumor) the comparisons data between the resection of edema and hemorrhagic necrosis areas need to be further examined in future studies. Analysis of contrast enhanced DSC and DCE perfusion studies can also be considered as a novel study. in addition, we did not make a combination of the three sequences. In the next step, researchers can fuse the three sequences'3D ROI and analyze them.

6. Conclusion

MRI texture analysis can be used as a new non-invasive method for the identification of gliomas with IDH1 mutation. The present results show that the Joint Variable derived from conventional MR imaging histogram and GLCM features can be used for precise detection of IDH1-mutated gliomas.

Conflict of interest

The authors declare no conflict of interest

Acknowledgment

This study was supported by the National Natural Science Foundation of China under grants 81671646.

References

[1] H. Yan, D.W. Parsons, G. Jin, et al., IDH1 and IDH2 mutations in gliomas, N. Engl. J. Med. 360 (8) (2009) 765–773.
[2] M. Sanson, Y. Marie, S. Paris, et al., Isocitrate dehydrogenase 1 codon 132 mutation is an important prognostic biomarker in gliomas, J. Clin. Oncol. 27 (25) (2009) 4150–4154.
[3] J. Beiko, D. Suki, K.R. Hess, et al., IDH1 mutant malignant astrocytomas aremore amenable to surgical resection and have a survival beneft associated with maximal surgical resection, Neuro Oncol. 16 (1) (2014) 81–91.
[4] M. Bujko, P. Kober, E. Matyja, et al., Prognostic value of IDH1 mutations identified with PCR-RFLP assay in glioblastoma patients, Mol. Diagn. Ther. 14 (3) (2010) 163–169.
[5] B.M. Ellingson, Radiogenomics and imaging phenotypes in glioblastoma: novel observations and correlation with molecular characteristics, Curr. Neurol. Neurosci. Rep. 15 (1) (2015) 506.
[6] J. Xiong, W.L. Tan, J.W. Pan, et al., Detecting isocitrate dehydrogenase gene mutations in oligodendroglial tumors using diffusion tensor imaging metrics and their correlations with proliferation and microvascular density, J. Magn. Reson. Imaging 43 (1) (2016) 45–54.
[7] K. Yamashita, A. Hiwatashi, O. Togao, et al., MR imaging-based analysis of glioblastoma multiforme:estimation of IDH1 mutation status, AJNR Am. J. Neuroradiol. 37 (1) (2016) 58–65.
[8] S. Bisdas, H. Shen, S. Thust, Texture analysis- and support vector machine-assisted diffusional kurtosis imaging may allow in vivo gliomas grading and IDH-mutation status prediction: a preliminary study, Sci. Rep. 8 (1) (2018) 6108.
[9] A.S. Jakola, Y.H. Zhang, A.J. Skjulsvik, et al., Quantitative texture analysis in the prediction of IDH status in low-grade gliomas, Clin. Neurol. Neurosurg. 164 (2018) 114–120.
[10] B.C. Christensen, A.A. Smith, S. Zheng, et al., DNA methylation, isocitrate dehydrogenase mutation, and survival in glioma, J. Natl. Cancer Inst. 103 (2) (2011) 143–153.
[11] C. Houillier, X. Wang, G. Kaloshi, et al., IDH1 or IDH2 mutations predict longer survival and response to temozolomide in low-grade gliomas, Neurology 75 (17) (2010) 1560–1566.
[12] H. Yang, D. Ye, K.L. Guan, Y. Xiong, IDH1 and IDH2 mutations in tumorigenesis: mechanistic insights and clinical perspectives, Clin. Cancer Res. 18 (20) (2012) 5562–5571.
[13] W. Xu, H. Yang, Y. Liu, et al., Oncometabolite 2-hydroxyglutarate is a competitive inhibitor of α-ketoglutarate-dependent dioxygenases, Cancer Cell 19 (1) (2011) 17–30.
[14] S.H.I. Jk, Y.L. Zhao, et al., The expression of IDH1 (R132H) is positively correlated with cell proliferation and angiogenesis in glioma samples, Chin. J. Cell Mol. Immunol. 32 (3) (2016) 360–363.
[15] D. Rohle, J. Popovici-Muller, N. Palaskas, An inhibitor of mutant IDH1 delays growth and promotes differentiation of glioma cells, Science 340 (6132) (2013) 626–630.
[16] Y.D. Zhang, Q. Wang, C.J. Wu, et al., The histogram analysis of diffusion-weighted intravoxel incoherent motion (IVIM) imaging for differentiating the gleason grade of prostate cancer, Eur. Radiol. 25 (4) (2015) 994–1004.
[17] S.T. Suo, X.X. Chen, Y. Fan, et al., Histogram analysis of apparent diffusion coefficient at 3.0T inurinary bladder lesions: correlation with pathologic fndings, Acad. Radiol. 21 (8) (2014) 1027–1034.
[18] H.J. Baek, H.S. Kim, N. Kim, et al., Percent change of perfusion skewness and kurtosis: a potential imaging biomarker for early treatment response in patients with newly diagnosed glioblastomas, Radiology 264 (3) (2012) 834–843.
[19] Y.Y. Wang, K. Wang, S.W. Li, et al., Patterns of tumor contrast enhancement predict the prognosis of anaplastic gliomas with IDH1 mutation, AJNR Am. J. Neuroradiol. 36 (11) (2015) 2023–2029.
[20] S. Zhao, Y. Lin, W. Xu, et al., Glioma-derived mutations in IDH1 dominantly inhibit IDH1 catalytic activity and induce HIF-1alpha, Science 324 (5924) (2009) 261–265.
[21] N. Rohwer, C. Zasada, S. Kempa, et al., The growing complexity of HIF-1α'srole in tumorigenesis: DNA repair and beyond, Oncogene 32 (31) (2013) 3569–3576.
[22] L. Ludemann, W. Grieger, R. Wurm, et al., Comparison of dynamic contrast-enhanced MRI withWHO tumor grading for gliomas, Eur. Radiol. 11 (2001) 1231.
[23] H. Hu, Z. Wang, Y. Liu, et al., Genome-wide transcriptional analyses of Chinese patients reveal cell migration is attenuated in IDH1-mutant glioblastoma, Cancer Lett. 57 (2) (2015) 566–574.